Solid State Science and Technology, Vol. 20, No 1 & 2 (2012) 128-133
ISSN 0128-7389

EFFECTS OF NANO-SiC ADDITION ON THE SUPERCONDUCTING PROPERTIES OF MAGNESIUM DIBORIDE

K.Y. Tan[1,*], K.L. Tan[1], K.B. Tan[2], K.P. Lim[1], S.A. Halim[1] and S.K. Chen[1]

[1]*Department of Physics, Universiti Putra Malaysia, UPM Serdang, Selangor.*

[2]*Department of Chemistry, Universiti Putra Malaysia, UPM Serdang, Selangor.*

**Corresponding author: kweeyong@gmail.com*

ABSTRACT

In this study, we report the results on phase formation, microstructures, and superconducting properties of a series of MgB_2 samples with different level of SiC additions. The polycrystalline samples were prepared via solid state reaction by mixing magnesium, boron and silicone carbide powders according to the ratio of Mg:B:SiC = 1:2:*x*. XRD spectra showed that MgB_2 is the primary phase while Mg_2Si, MgO and MgB_4, together with some unreacted SiC are the secondary phases as the addition increases. The presence of Mg_2Si became more significant as the addition level increased. SEM images showed smaller grains as the addition level increases indicating more grain boundaries were formed. The T_c was as low as 30.5K for *x*=15wt%. The field dependence of J_c showed that *x*=1wt% sample gave the best performance at both 5K and 20K.

Keywords: MgB_2; MgO; MgB_4; superconducting properties

INTRODUCTION

The discovery of magnesium diboride (MgB_2) as a superconductor by J. Akimitsu has attracted researchers to involve themselves so as to further study this compound and to enhance its superconducting properties [[1]. Typical methods such as chemical doping and variation of stoichiometry has been employed to improve its properties for high field applications [1],2]. So far, various dopants have been used, such as SiC [3-5], Copper [6], and Carbon [5,7]. Previous reports show that SiC doping has yielded J_c as high as ~10^8 A/cm^2 for thin films [2]. Thus, it is obvious the use of SiC as a dopant is able to enhance the current carrying capability of MgB_2. Moreover, smaller particle size of dopant is easier to incorporate into the grains and serve as effective pinning centers [8]. Due to the low melting point of Mg, special cares are necessary to prevent Mg loss or Mg oxidation. By choosing a lower sintering temperature, grain growth will be limited giving rise to the formation of more grain boundaries [9-10]. In this work, different weight percentages of nano-SiC was added into MgB_2 and their effects on the superconducting properties were investigated. Our aim is two-fold, i.e. reaction between Mg and SiC is expected to lead to the formation of Mg_2Si precipitates in MgB_2 matrix to serve as pinning centers while the release of C from the same reaction would

Solid State Science and Technology, Vol. 20, No 1 & 2 (2012) 128-133
ISSN 0128-7389

substitute the boron site. The use of nano-size SiC accelerates its reaction rate with Mg.

METHODS

The samples were prepared via *in-situ* solid state reaction method using magnesium (Tangshan, 99%), amorphous boron (Pfaltz&Bauer, 99%) and nano-silicone carbide (Nano-Amor, 15nm, 99+%). These powders were weighed according to the stoichiometric ratio of Mg:B:SiC = 1:2:x where x = 0, 1, 5, 10 and 15wt% relative to the weight of the MgB_2 samples prepared. After a thorough mixing for 2 hours, the mixture was then pressed into 13mm diameter pellets. In order to minimize the contact with sintering atmosphere, the pellets were sealed inside SUS306 stainless steel tubes. Argon gas was subsequently flown through the furnace during the sintering process. The pellets were sintered at 850°C for 1 hr with the heating and cooling rates of 10°C/min. The samples were analyzed by using X'Pert Pro Panalytical PW3040 MPD X-ray Diffractometer with Cu anode. The microstructures were studied by using JEOL JSM 6400 Scanning Electron Microscope (SEM) equipped with EDX. T_c and J_c measurements were carried out by using a Quantum Design-Magnetic Property Measurement System (MPMS).

RESULTS AND DISCUSSION

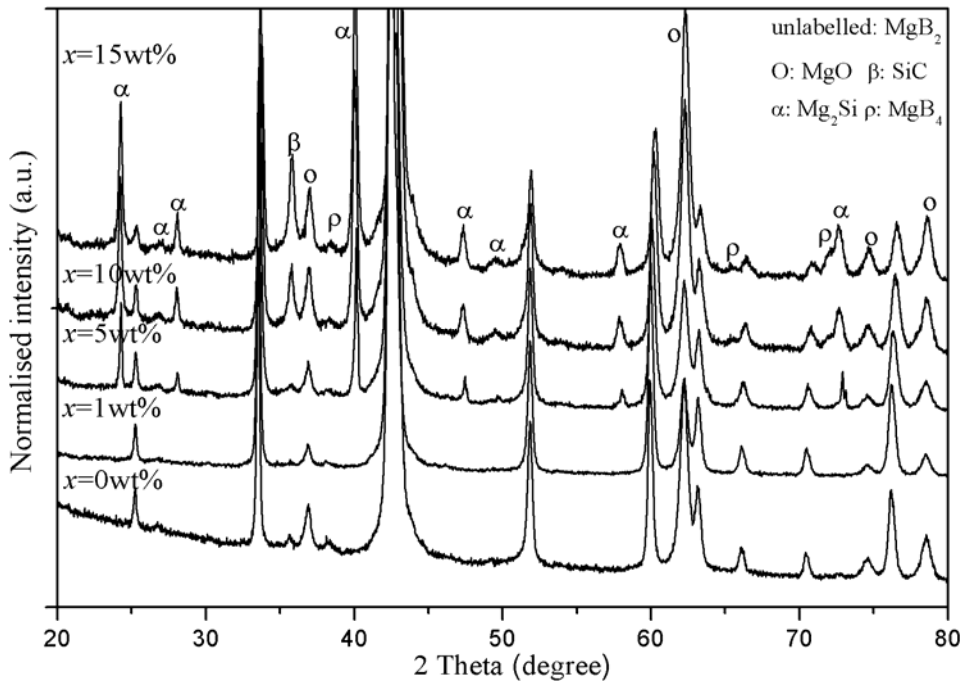

Figure 1: XRD spectra of various level of SiC added MgB_2

Figure 1 shows the XRD spectra of MgB_2 samples with various level of SiC additions. The existence of MgO peaks is obvious because of residual oxygen, which was hard to be eliminated and was entrapped inside the stainless steel tube even before sintering.

Table 1 shows the MgO relative intensity fractions of the samples. The relative intensity fraction of MgO was calculated according to ref. [11]. Small amount of nano-SiC addition was actually an aid in reducing the MgO phase as the MgO relative intensity fraction of 1wt% and 5wt% were lower than that of the pure sample. The increase in MgO with SiC addition level may be attributed to some of the oxidized nano-SiC particles that led to the oxidation of Mg.

Table 1: Various parameters of different level addition of SiC in MgB_2

Addition level (wt%)	$FWHM_{001}$	$FWHM_{110}$	Density (g/cm^3)	Density Ratio	MgO Relative Intensity Fraction (%)
0	0.1224	0.2244	1.4099	0.5529	8.5
1	0.1836	0.2040	1.4073	0.5519	3.8
5	0.2040	0.0816	1.4112	0.5534	5.7
10	0.2040	0.2448	1.4248	0.5587	10.0
15	0.2448	0.3672	1.3852	0.5432	14.7

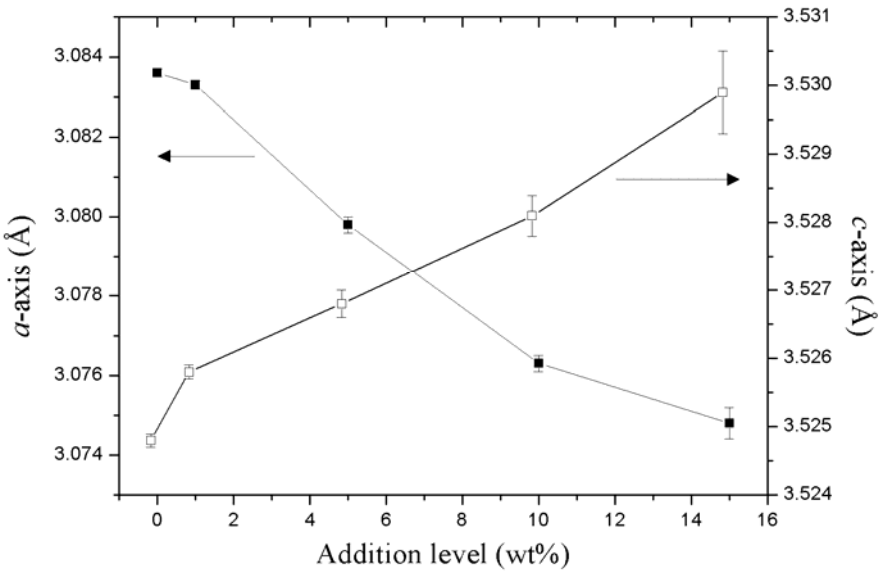

Figure 2: Evolution of lattice parameters with additions of SiC into MgB_2

As the level of nano-SiC increases, more Mg_2Si phase was formed in accordance to previous reports [8,12]. MgB_4 was also observed in the spectra for x=10wt% and 15wt% because of Mg deficiency. Unreacted nano-SiC was observed in MgB_2 for x=5wt%, 10wt% and 15wt%. It is known that the variation in full width half maximum (FWHM) can be related to the lattice distortion or changes in crystallinity [5]. As shown in Table 1, the increase of FWHM can be due to the C-doping at B-site. This is also evidenced from Figure 2 showing larger *c-axis* and smaller *a-axis* with addition of SiC

supporting C-doping has taken place at B-site when addition increased and distorted the original MgB_2 structure. This is also consistent with previous reports that *a-axis* shortens whereas *c-axis* is either elongated or unchanged as the addition of SiC increases [8]. The density ratio shown in Table 1 was obtained by calculating the sample density over the theoretical density of MgB_2 (~2.55g/cm^3). It is clear that additions of SiC into MgB_2 did not assist the increase of sample density. Generally, the samples only attained about half of the theoretical density [12].

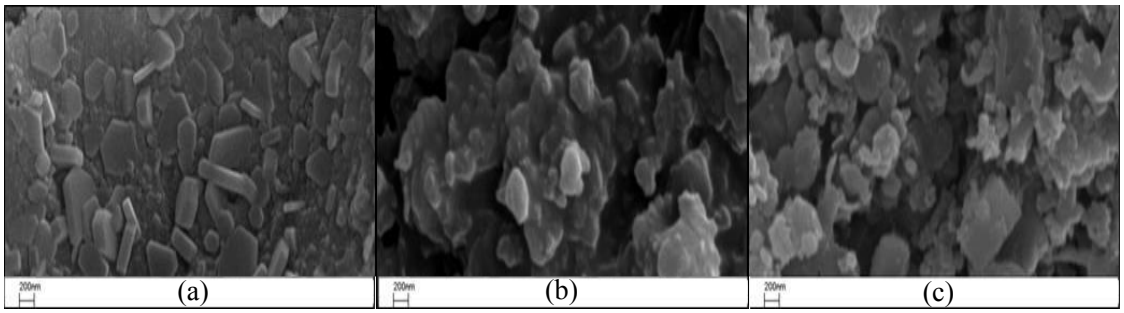

Figure 3: SEM images of (a) pure MgB_2, (b) 5wt% SiC added MgB_2, (c) 10wt% SiC added MgB_2

Figure 3 shows the SEM images of pure MgB_2 (a), 5wt% SiC added MgB_2 (b), 10wt% SiC added MgB_2 (c) magnified at 20k. The pure sample was observed to show clear hexagonal shape grains with the size in the range of about 200 - 400nm. Some of the grains with smaller size of 100nm can also be seen in 5wt% SiC added MgB_2, thus, creating more grain boundaries. The average grain size is approximately 300nm in this sample. As the nano-SiC addition increased to 10wt%, the grains can be observed to agglomerate. There are more grains in the size of as small as 50nm. Some of the smaller grains are possibly unreacted nano-SiC and Mg_2Si which could serve as pinning centres [9].

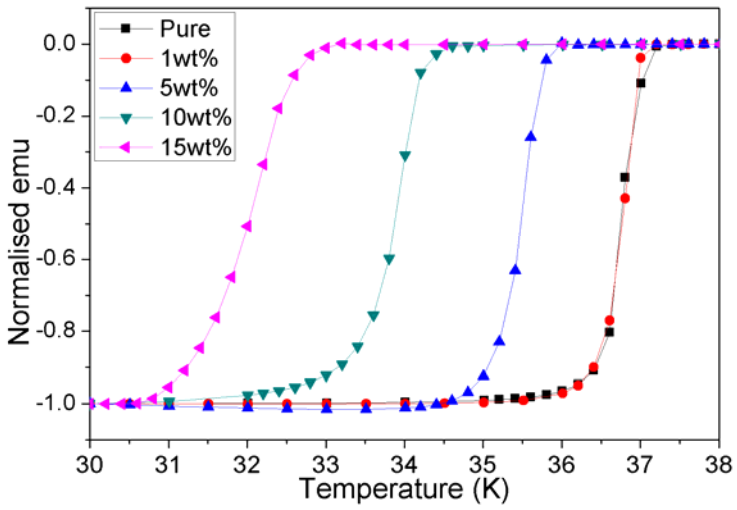

Figure 4: T_c of various SiC addition level added MgB_2

Figure 4 shows the transition temperature (T_c) of the MgB_2 samples with different level of SiC additions. The plot shows that the T_c of the samples drops gradually as the addition level increases and it is as low as 30.5K for the 15wt% SiC additions, i.e. about 5.5K of decrease compared to the T_c of pure sample (36K). The transition width, ΔT, of the samples increases slowly with the addition of the nano-SiC as shown in Figure 4. The increase in ΔT is in agreement with the XRD spectra (Figure 1) showing the increase in impurities with SiC addition. The B-plane in MgB_2 plays a main role in its superconductivity and the substitution of C at B-site disturbs the lattice structure. By increasing the addition level of SiC, T_c of the samples is reduced and ΔT increases with shortening in *a-axis* as shown in Figure 2.

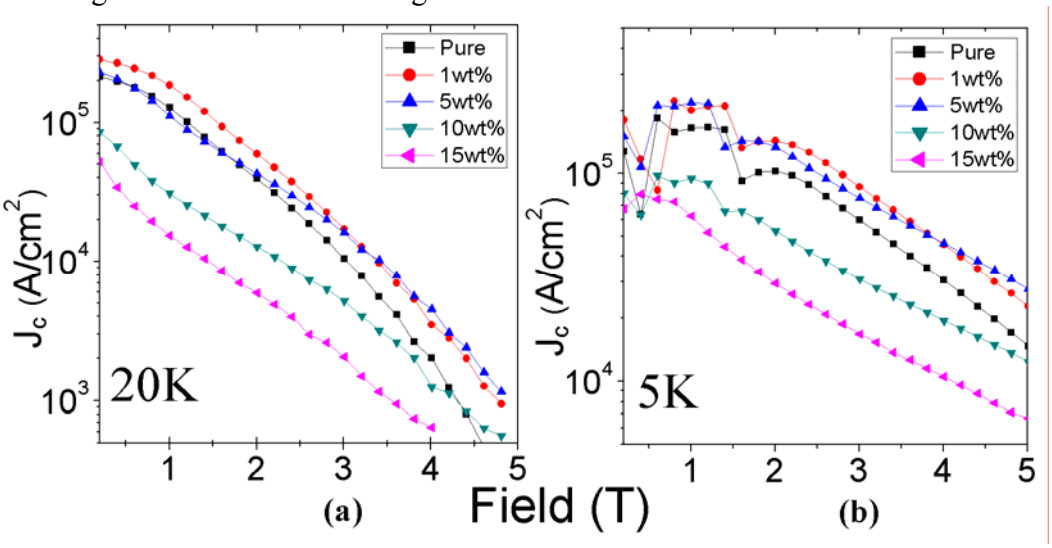

Figure 5: J_c of various SiC addition level added MgB_2 at 20K(a), and 5K (b)

Figure 5 shows the critical current density plots for 5K and 20K. Both of the plots show improvement in J_c for 1wt% and 5wt% nano-SiC added samples. At 20K and 2T, J_c of the 1wt% added sample is 6×10^4 A/cm^2 and this value is even higher at 1.5×10^5 A/cm^2 for 5K. The results show nearly 50% improvements at 5K, 2T and 20K, 2T compared to pure samples. However, as the field increases, 5wt% added sample show better J_c performance than 1wt% added sample starting at 3T for 20K and 4.1T for 5K. Although the 10wt% and 15wt% added samples shows lower J_c than pure sample for both 5K and 20K but the drop of J_c of the formers is more gradual. The improvement in J_c can be credited to the secondary phases of unreacted nano-SiC and Mg_2Si which serve as effective flux pinning centre. Besides, slower drop of J_c especially in high field is expected in 10wt% and 15wt% added samples due to additional grain boundary pinning because of smaller grains as shown by SEM images.

CONCLUSIONS

The effects of nano-SiC additions into MgB_2 on the phase formation, microstructure and superconducting properties were evaluated. As nano-SiC addition increases, more

secondary phases are present, especially Mg_2Si and MgB_4 and the crystallinity of the samples decreases. SEM shows smaller grains in samples with higher level of SiC addition. The T_c was found to decrease from 36K for the pure sample to 30.5K for sample with x=15wt%. However, a significant improvement of near 50% in J_c was recorded as high as 1.5×10^5 A/cm^2 at 5K, 2T for 1wt% added samples compare to pure sample. Thus, appropriate nano-SiC addition is a promising mean for enhancing the J_c performance of MgB_2.

ACKNOWLEDGMENT

The authors would like to acknowledge the financial support from The Ministry of Science, Technology and Innovation Malaysia (MOSTI) under the Science Fund 03-01-04-SF0920.

REFERENCES

[1] J. Nagamatsu, N. Nakagawa, T. Muranaka, Y. Zenitani, J. Akimitsu, *Nature*. **410** (2001) 63-64
[2] X. X. Xi, *Rep. Prog. Phys.*, **71** (2008) 116501
[3] O. Husnjak, I. Kušević, E. Babić, S. Soltanian, X.L. Wang, S.X. Dou, *Physica C* **460–462** (2007) 591–592
[4] C.H. Jiang, T. Nakane, H. Kumakura, *Physica C* **436** (2006) 118–122
[5] J.H. Lim, S.H. Jang, S.M. Hwang, J.H. Choi, J. Joo, W.N. Kang, C. Kim, *Physica C* **468** (2008) 1829–1832
[6] S. K. Chen, M. Majoros, J. L. MacManus-Driscoll, B. A. Glowacki, *Physica C* **418** (2005) 99-106
[7] M. Mudgel, V.P.S. Awana, H. Kishan, G.L. Bhalla, *Solid State Comm.* **146** (2008) 330–334
[8] A. Yamamoto, J. Shimoyama, I. Iwayama, Y. Katsura, S. Horii, K. Kishio, *Physica C* **463-365** (2007) 807-811
[9] A. Yamamoto, J. Shimoyama, S. Ueda, Y. Katsura, S. Horii, K. Kishio, *Supercond. Sci. Technol.* **18** (2005) 116-121
[10] A. Yamamoto J. Shimoyama, S. Ueda, Y. Katsura, I. Iwayama, S. Horii, K. Kishio, *Physica C* **426-431** (2005) 1220-1224
[11] J. H. Kim, S.X. Dou, D. Q. Shi, M. Rindfleisch, M. Tomsic, *Supercond. Sci. Technol.* **20** (2007) 1026-1031
[12] S. X. Dou, A.V. Pan, S. Zhou, M. Ionescu, H. K. Liu, P. R. Munroe, *Supercond. Sci. Technol.* **15**, (2002) 1587-1591